Orthogonal Spectral Coding of Entangled Photons

Joseph M. Lukens,[1] Amir Dezfooliyan,[1] Carsten Langrock,[2] Martin M. Fejer,[2] Daniel E. Leaird,[1] and Andrew M. Weiner[1,*]
[1]School of Electrical and Computer Engineering, Purdue University, West Lafayette, Indiana 47907, USA
[2]E. L. Ginzton Laboratory, Stanford University, Stanford, California 94305, USA
(Received 2 December 2013; published 1 April 2014)

We extend orthogonal optical coding, previously applied to multiuser classical communication networks, to entangled photons. Using a pulse shaper and sum-frequency generation for ultrafast coincidence detection, we demonstrate encoding and decoding of biphoton wave packets. Applying one code to the signal photon spreads the wave packet in time and creates a null at zero delay; filtering the idler with the matched code recovers a narrow correlation peak, whereas applying any other code leaves the wave packet spread. Our results could prove useful in the development of code-based quantum communication networks.

DOI: 10.1103/PhysRevLett.112.133602 PACS numbers: 42.50.Dv, 03.67.-a, 42.65.Ky, 42.65.Lm

Recently there has grown a significant interest in classical analogues of many foundational quantum optical phenomena, including Hong-Ou-Mandel interference [1–4] and Franson dispersion cancellation [5–9]. And even though the classical versions lack entanglement, they can at times offer significant advantages over their quantum counterparts. For example, chirped-pulse interferometry [3] can achieve the same resolution improvement as quantum optical coherence tomography [10], but at classically high power levels. Several of these classical analogues are based on time-reversed versions of entanglement generation [3,4,9]. Instead of using spontaneous parametric down-conversion (SPDC) of a narrow-band pump to generate broadband entangled photons, similar effects can be seen by considering instead sum-frequency generation (SFG) of broadband classical fields at a fixed up-conversion frequency. This process effectively postselects only the spectral combinations of the classical field that are correlated in the same manner as entangled photons.

Alternatively, the field of Fourier pulse shaping [11] has bridged the gap between quantum and classical realizations in the opposite direction; considered originally for coherent classical pulses, it has recently been extended to the shaping of biphoton correlations as well [12–15]. Expanding on these results in pulse shaping, and exploiting the operational similarities between classical narrow-band SFG and entangled photons, we experimentally study a new biphoton coding scheme based on spectral orthogonality, previously utilized in classical optical code-division multiple access [16,17]. Our results establish a novel method for the encoding of information in the spectral degree of freedom of biphotons, with the potential for application not only in implementing multiuser quantum key distribution (QKD) [18], but also in the development of new code-based time-frequency QKD protocols, as alternatives to previous proposals based on dispersion [19] or temporal modulation [20].

The foundation for many optical code-division multiple access realizations is some set of orthogonal codes, at least as numerous as the number of users on the network. So-called Hadamard codes (designations "Walsh" and "Walsh-Hadamard" are also common [21]) are a convenient choice. A given family consists of N length-N sequences of ones and minus ones, or, equivalently, phases of 0 and π; each element of a given sequence is traditionally called a "chip." These codes have the property that any two different sequences are orthogonal. That is, if we describe code m and n by the corresponding vectors $\mathbf{v}_m$ and $\mathbf{v}_n$, respectively, we have

$$\mathbf{v}_m \cdot \mathbf{v}_n = N\delta_{mn}, \tag{1}$$

where δ_{mn} is the Kronecker delta, equal to unity if $m = n$, and zero otherwise. We mention here relevant work involving spectral coding of coherent optical pulses, in which one code is applied to half of the spectrum, and a second one to the other half; then a narrow-band SFG field is generated and measured [22,23]. Presuming that phase matching permits all constituent frequencies to combine, the generated SFG field at frequency $2\omega_0$, $E_{\mathrm{SFG}}(2\omega_0)$, is given by the integral [24]

$$E_{\mathrm{SFG}}(2\omega_0) \propto \int_0^\infty d\Omega E(\omega_0 + \Omega)E(\omega_0 - \Omega). \tag{2}$$

For an input field with a flat spectral amplitude, the integral can be viewed as the inner product between the Hadamard codes applied to each half of the spectrum. If they are identical (i.e., a mirror image about ω_0), a high yield is found, but if they differ, orthogonality ensures that the integral drops to zero. This discrimination provides a means for many users to communicate over the same spectrotemporal space. The sender encodes the message by applying the intended receiver's code to one spectral half, and only

the receiver who applies the correct code to the opposite half will see the message above the background.

The quantum version which we present relies on the intrinsic spectral correlation of entangled photons, the time-reversed version of classical SFG [3,4,9]. Considering degenerate down-conversion of a monochromatic pump beam at frequency $2\omega_0$, the biphoton state can be approximated as

$$|\Psi\rangle = M|\mathrm{vac}\rangle_s|\mathrm{vac}\rangle_i + \int_0^\infty d\Omega\phi(\Omega)|\omega_0+\Omega\rangle_s|\omega_0-\Omega\rangle_i, \tag{3}$$

where $M \sim 1$, "vac" denotes the vacuum state, $\phi(\Omega)$ is determined by phase-matching conditions, and s and i represent the signal and idler, respectively [25]. Applying the spectral filter $H_s(\omega)$ to the signal and $H_i(\omega)$ to the idler, we obtain the output biphoton wave packet

$$\psi(t+\tau,t) \propto \int_0^\infty d\Omega\phi(\Omega)H_s(\omega_0+\Omega)H_i(\omega_0-\Omega)e^{-i\Omega\tau}, \tag{4}$$

the modulus squared of which gives the probability density for detecting the signal photon a time τ after the idler. If $\phi(\Omega)$ is essentially flat over the frequencies considered, and the spectral filters correspond to Hadamard codes, we have precisely the situation in Eq. (2) at $\tau = 0$: matched codes give a peak, whereas mismatched codes yield essentially zero. How such coding on entangled photons would work is summarized in Fig. 1. The signal half of the spectrum corresponding to a temporally narrow biphoton is initially encoded with a sequence of 0 and π phases, which spreads and lowers the temporal correlation function, creating a null at zero delay. Then a second phase code is applied to the idler. If the codes match in the symmetric sense, the sharply peaked biphoton is recovered, with a temporal shape identical to the uncoded biphoton in the ideal case. But if the codes differ, the correlation function remains spread with zero magnitude at $\tau = 0$. We remark that this configuration can be viewed as the spectral dual to the temporal coding demonstrated in Ref. [26].

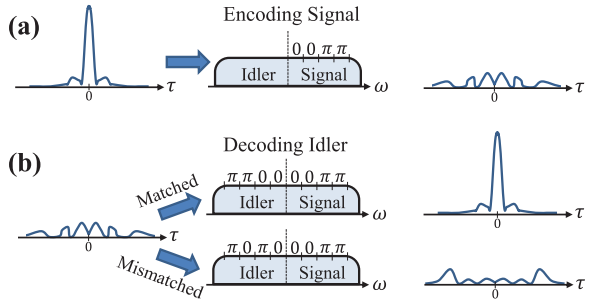

FIG. 1 (color online). Principle of biphoton spectral coding. (a) Encoding the biphoton. A sequence of 0 and π phase shifts is applied to the signal half-spectrum of a temporally narrow biphoton, which spreads the correlation function in time and produces a null at $\tau = 0$. (b) Decoding the biphoton. A second code is applied to the idler half of the spectrum. If it matches that used for encoding, the narrow correlation peak is recovered, while an unmatched code instead leaves the correlation function in a new, but still spread, state.

For a more intuitive understanding of our approach, one can describe this encoding and decoding phenomenon as an example of the quantum mechanical interference of indistinguishable paths. Unlike classical probabilities, the complex amplitudes associated with quantum paths interfere with each other if they cannot be distinguished, even in principle [27]. Several definitive examples of two-photon interference, such as Hong-Ou-Mandel [1] and Franson [28], can be viewed as the interference of two indistinguishable quantum mechanical paths. In our orthogonal coding case, we instead have N indistinguishable bin combinations of frequency pairs, for without additional measurements that destroy the experiment, it is impossible to tell through which Hadamard chips the detected photons passed. Accordingly, the probability amplitudes interfere with each other, and when mismatched codes give identical numbers of pair offsets with combined phase shifts of 0 and π, we obtain perfect cancellation at zero delay. Thus one can view our orthogonal coding approach as an extension of path interference in which the number of paths is programmably controlled by a pulse shaper.

This flexibility in choosing the dimensionality of the coding process—and, indeed, the effectiveness of the coding itself—derives from the high degree of entanglement possessed by our biphoton source. In general, bipartite entanglement is quantified by the Schmidt number, which roughly corresponds to the total signal-idler spectral modes contributing to the entanglement [29,30]. The Schmidt decomposition conveys the information potential of an entangled photon pair, indicating in our scheme the maximum useful code dimensionality and also conceivably limiting the spectral shapes of correlated signal-idler frequency modes. Experimentally, this degree of entanglement is well characterized by the Fedorov parameter [31], or the ratio of the marginal signal bandwidth to that conditioned on a frequency measurement of the idler. For our source, with a total signal bandwidth over 2 THz and a conditional width predicted to be less than 200 kHz (the pump laser linewidth) the estimated Fedorov ratio is in excess of 10 million. Such high-dimensional entanglement fully justifies the monochromatic pump assumption built into Eq. (3), and it also indicates that our coding process, which we push to a dimension of 40, is only beginning to access the intrinsic information potential of the biphotons themselves; as we note later, experimental limitations such as pulse-shaper resolution prove far more restrictive.

Our experimental setup is given in Fig. 2. We couple about 16 mW of a 774-nm pump laser into a periodically

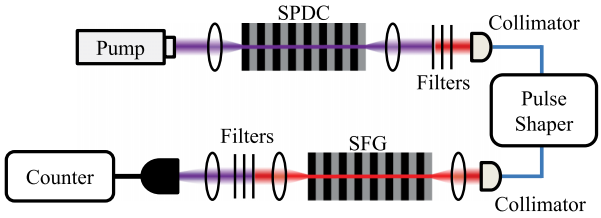

FIG. 2 (color online). Experimental setup. High-frequency photons at 774 nm decay into entangled photons through SPDC in a PPLN waveguide. The pump is filtered out and the biphotons coupled into optical fiber, in which a pulse shaper is used to manipulate the spectrum and apply delay between the signal and idler photons. The photons are then recombined via SFG in a second PPLN waveguide, which acts as an ultrafast optical gate for measuring coincidences.

poled lithium niobate (PPLN) waveguide [32], which generates entangled pairs through SPDC with an internal efficiency of about 10^{-5} per coupled photon. The residual pump is removed with filters and the biphotons coupled into optical fiber. A commercial pulse shaper (Finisar WaveShaper 1000S) distinguishes signal and idler by frequency and applies the spectral codes. The power spectrum of the SPDC emission [33] varies by less than 0.8 dB over the 2.4-THz signal and idler passbands set by the pulse shaper, which ensures that all Hadamard chips contribute with approximately equal weight, a necessary condition to achieve orthogonality. The pulse shaper also compensates for fiber dispersion and can impose a relative delay between signal and idler for subsequent measurements of the temporal correlation function. The photons are then coupled into a second PPLN waveguide and, provided they temporally overlap, can recombine via SFG into a single photon at 774 nm; the measured internal efficiency for this process is 10^{-5} with optimal alignment. When the phase-matching conditions allow all entangled frequency pairs to combine with equal probability, the flux of SFG photons at each delay step directly measures the temporal correlation function on a femtosecond time scale, as first shown in Ref. [12]. More details regarding our experimental setup, as well as confirmation of operation in the single-pair regime, are provided in Ref. [33].

While we do employ an SFG detection scheme in these experiments, just as in the classical version [22,23], our use is fundamentally different. In the classical implementation, the process of narrow-band SFG is necessary to achieve the desired spectral gating of the product of the input fields—up-conversion evaluates only the waveform corresponding to the Hadamard products. But in our case, SFG is required only inasmuch as it furnishes sufficient timing resolution to observe the fine features of the correlation function. The orthogonality condition is imposed on the biphoton state itself and therefore could be seen nonlocally by isolated detectors possessing adequate resolution. Thus, our use of SFG is not a fundamental, but only technical restriction which could be removed in the future by improvements in single-photon detector jitter to the picosecond level [34].

We first examine the utility of our biphoton phase codes by testing the orthogonality of several length-N Hadamard families, measuring the count rate at zero delay for all possible code combinations. In a previous work [35], we demonstrated an alternative amplitude coding method, in which the maximum contrast between matched and mismatched cases is 2:1. Here, however, utilizing pure phase coding accompanied by ultrafast coincidence detection, the contrast between the coincidences at zero delay for matched and mismatched codes is ideally unbounded. Experimentally, we have considered code lengths of 4, 8, 20, and 40 (chip bandwidths of 600, 300, 120, and 60 GHz, respectively); the average measured contrast is 40:1 in the $N = 4$ case, 59:1 for $N = 8$, 115:1 for $N = 20$, and 49:1 for $N = 40$, limited primarily by accidentals and alignment stability.

The full results for the length-20 and length-40 cases are provided in Figs. 3(a) and 3(b), showing visually the sharp discrimination for matched codes. The higher count rates for code 1 in both plots, as well as for code 21 in the length-40 case, are fully explained by theory. Because of the finite pulse-shaper resolution, sharp phase transitions from 0 to π introduce diffractive losses, a well-known effect in classical pulse shaping [24]. Since the first code possesses no such transitions (it consists entirely of zero-phase chips), and code 21 of Fig. 3(b) has only one transition, the net count

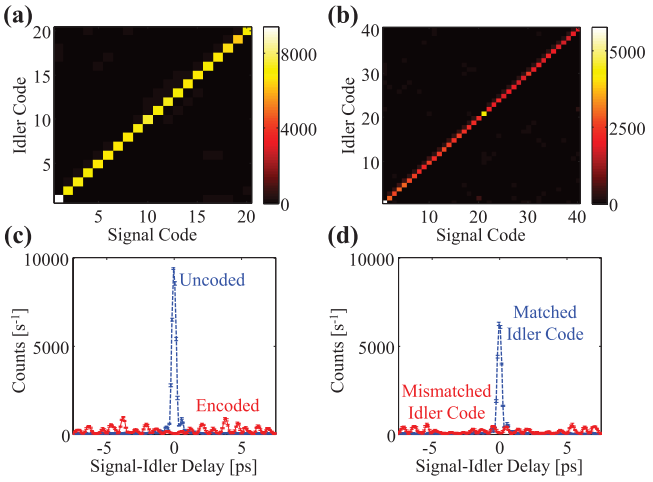

FIG. 3 (color online). Hadamard orthogonality for long sequences. (a) Measured coincidences [s^{-1}] at zero optical delay for all combinations in the $N = 20$ code family. (b) Coincidence map for length-40 codes. (c),(d) Specific example of length-40 coding. (c) With no codes applied, a sharp correlation function is measured, but when code 28 is applied to the signal, the peak disappears and the biphoton spreads. (d) Applying code 28 to the idler recovers the sharp correlation function, yet programming the wrong code (in this case, code 3) keeps the biphoton spread. Error bars give the standard deviation of five 1-s measurements, after dark count subtraction.

rate after the coding and decoding process is appreciably higher for these cases than in the other codes with multiple π phase jumps.

To highlight the biphoton coding picture presented in Fig. 1, we also acquire full correlation functions for specific combinations in the length-40 Hadamard map. Figure 3(c) shows encoding of the signal photon using code 28 from the two-dimensional map. For flat phase applied to both signal and idler, the correlation function possesses a narrow peak exceeding 9000 s^{-1} in measured coincidences. [The peak surpasses that in Fig. 3(b) due to alignment reoptimization.] When code 28 is applied to the signal, the waveform spreads, and only about 30 s^{-1} are measured at zero delay. The decoding process is verified in Fig. 3(d): applying code 3 to the idler keeps the correlation function spread, with a zero-delay SFG count rate of only about 60 s^{-1}, whereas when code 28 is applied, the biphoton regains its sharp peak. The height of the decoded peak is reduced to about two thirds that of the uncoded case, which again is in agreement with the expected drop from pulse-shaper resolution. These results confirm the conceptual picture of Fig. 1, showing that we can indeed hide and recover a biphoton wave packet in our coding scheme. Moreover, the fact that pulse-shaper resolution limits the maximum code length that can be implemented—introducing loss and waveform degradation as the chip bandwidth decreases—mirrors similar findings in orbital angular momentum, in which experimental imperfections have been shown to fix an optimum dimension beyond which the secure information capacity drops [36]. Proper code-length selection will therefore play an important role in developing our spectral coding approach in the context of QKD.

Finally, while most Hadamard code combinations give results that appear essentially featureless, certain specializations can yield interesting wave packets in their own right. For example, choosing a code of alternating 0's and π's for the signal and flat phase for the idler, we once again obtain orthogonality at zero delay, suppressing the correlation function peak. However, the pattern's periodic nature yields values of optical delay for which the biphoton packet can display large maxima. For a chip bandwidth of $\Delta\omega$, every other $\Delta\omega$ bin pair picks up a π phase shift, but as can be seen in Eq. (4), for delays $\tau = \pm\pi/\Delta\omega$, each bin acquires an additional spectral phase of 0, π, 2π, 3π, etc., which precisely compensates for the alternating pattern and allows each frequency pair to interfere constructively, producing a temporal peak. Additional local maxima surface at all odd multiples of the above delay, but the finite chip bandwidth suppresses them so that most of the optical energy is concentrated in the first two peaks about zero. This particular code therefore converts a single correlation peak into a doublet, with separation controlled by the chip rate. Figure 4 furnishes experimental examples, for 240- and 100-GHz chips. Theory is confirmed, as the generated

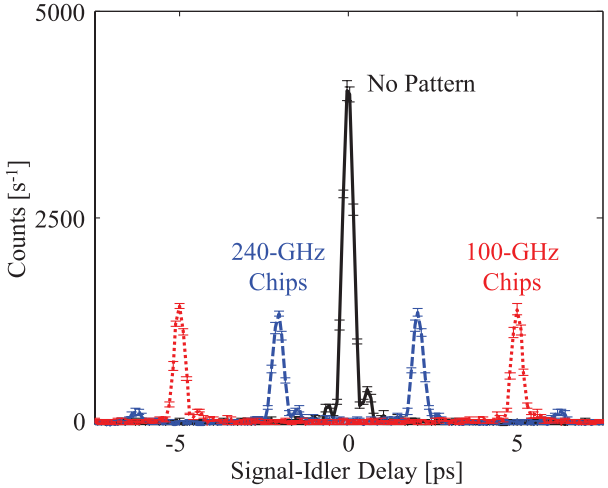

FIG. 4 (color online). Correlation doublet creation. The length-10 pattern, with 240-GHz chips, creates a separation of 4.2 ps; the length-24 pattern, comprised of 100-GHz chips, increases this separation to 10 ps. Again, error bars show the standard deviation of five 1-s measurements, with dark counts subtracted.

peaks appear at ± 2.1 and ± 5 ps, respectively. Two subsidiary maxima are even discernible at ± 6.3 ps for the 240-GHz case, matching the odd-multiple prediction. These findings provide just one example of the possibilities available for biphoton manipulation based on optical codes.

This work was funded by the Office of Naval Research under Grant No. N000141210488. J. M. L. acknowledges financial support from the Department of Defense through a National Defense Science and Engineering Graduate Fellowship.

*amw@purdue.edu

[1] C. K. Hong, Z. Y. Ou, and L. Mandel, Phys. Rev. Lett. **59**, 2044 (1987).
[2] B. I. Erkmen and J. H. Shapiro, Phys. Rev. A **74**, 041601 (2006).
[3] R. Kaltenbaek, J. Lavoie, D. N. Biggerstaff, and K. J. Resch, Nat. Phys. **4**, 864 (2008).
[4] R. Kaltenbaek, J. Lavoie, and K. J. Resch, Phys. Rev. Lett. **102**, 243601 (2009).
[5] J. D. Franson, Phys. Rev. A **45**, 3126 (1992).
[6] V. Torres-Company, H. Lajunen, and A. T. Friberg, New J. Phys. **11**, 063041 (2009).
[7] J. H. Shapiro, Phys. Rev. A **81**, 023824 (2010).
[8] V. Torres-Company, J. P. Torres, and A. T. Friberg, Phys. Rev. Lett. **109**, 243905 (2012).
[9] R. Prevedel, K. M. Schreiter, J. Lavoie, and K. J. Resch, Phys. Rev. A **84**, 051803 (2011).
[10] A. F. Abouraddy, M. B. Nasr, B. E. A. Saleh, A. V. Sergienko, and M. C. Teich, Phys. Rev. A **65**, 053817 (2002).
[11] A. M. Weiner, Opt. Commun. **284**, 3669 (2011).
[12] A. Pe'er, B. Dayan, A. A. Friesem, and Y. Silberberg, Phys. Rev. Lett. **94**, 073601 (2005).

[13] B. Dayan, Y. Bromberg, I. Afek, and Y. Silberberg, Phys. Rev. A **75**, 043804 (2007).
[14] F. Zäh, M. Halder, and T. Feurer, Opt. Express **16**, 16452 (2008).
[15] E. Poem, Y. Gilead, Y. Lahini, and Y. Silberberg, Phys. Rev. A **86**, 023836 (2012).
[16] A. M. Weiner, Z. Jiang, and D. E. Leaird, J. Opt. Net. **6**, 728 (2007).
[17] J. P. Heritage and A. M. Weiner, IEEE J. Sel. Top. Quantum Electron. **13**, 1351 (2007).
[18] M. Razavi, IEEE Trans. Commun. **60**, 3071 (2012).
[19] J. Mower, Z. Zhang, P. Desjardins, C. Lee, J. H. Shapiro, and D. Englund, Phys. Rev. A **87**, 062322 (2013).
[20] J. Nunn, L. J. Wright, C. Söller, L. Zhang, I. A. Walmsley, and B. J. Smith, Opt. Express **21**, 15959 (2013).
[21] K. G. Beauchamp, *Applications of Walsh and Related Functions (Academic Press, London, 1984).*
[22] Z. Zheng and A. M. Weiner, Opt. Lett. **25**, 984 (2000).
[23] Z. Zheng, A. M. Weiner, K. R. Parameswaran, M.-H. Chou, and M. M. Fejer, IEEE Photonics Technol. Lett. **13**, 376 (2001).
[24] A. M. Weiner, *Ultrafast Optics (Wiley, Hoboken, NJ, 2009).*
[25] L. Mandel and E. Wolf, *Optical Coherence and Quantum Optics (Cambridge University Press, Cambridge, England, 1995).*
[26] C. Belthangady, C.-S. Chuu, I. A. Yu, G. Y. Yin, J. M. Kahn, and S. E. Harris, Phys. Rev. Lett. **104**, 223601 (2010).
[27] L. Mandel, Rev. Mod. Phys. **71**, S274 (1999).
[28] J. D. Franson, Phys. Rev. Lett. **62**, 2205 (1989).
[29] C. K. Law, I. A. Walmsley, and J. H. Eberly, Phys. Rev. Lett. **84**, 5304 (2000).
[30] C. K. Law and J. H. Eberly, Phys. Rev. Lett. **92**, 127903 (2004).
[31] M. V. Fedorov, M. A. Efremov, A. E. Kazakov, K. W. Chan, C. K. Law, and J. H. Eberly, Phys. Rev. A **69**, 052117 (2004).
[32] C. Langrock, S. Kumar, J. E. McGeehan, A. E. Willner, and M. M. Fejer, J. Lightwave Technol. **24**, 2579 (2006).
[33] J. M. Lukens, A. Dezfooliyan, C. Langrock, M. M. Fejer, D. E. Leaird, and A. M. Weiner, Phys. Rev. Lett. **111**, 193603 (2013).
[34] R. H. Hadfield, Nat. Photonics **3**, 696 (2009).
[35] J. M. Lukens, A. Dezfooliyan, C. Langrock, M. M. Fejer, D. E. Leaird, and A. M. Weiner, Opt. Lett. **38**, 4652 (2013).
[36] J. Leach, E. Bolduc, D. J. Gauthier, and R. W. Boyd, Phys. Rev. A **85**, 060304 (2012).